Constraints on $q\bar{q}\gamma\gamma$ Contact Interactions at Future Hadron Colliders

THOMAS G. RIZZO[1]

Stanford Linear Accelerator Center
Stanford University, Stanford, California 94309 USA

ABSTRACT

We explore the capability of the Tevatron and LHC as well as other future hadron colliders to place limits on the possible existence of flavor-independent $q\bar{q}\gamma\gamma$ contact interactions which can lead to an excess of high p_t diphoton events with large invariant masses. Constraints on the corresponding $e^+e^-\gamma\gamma$ contact interaction already exist from LEP. In the case of hadron colliders, strong constraints on the scale associated with such interactions are achievable in all cases, *e.g.*, of order 0.9(3) TeV at TeV33(LHC).

To appear in the *Proceedings of the 1996 DPF/DPB Summer Study on New Directions for High Energy Physics-Snowmass96*, Snowmass, CO, 25 June-12 July, 1996.

---

1   Introduction

Although the Standard Model(SM) appears to be as healthy as ever[1], it is generally believed that new physics must exist to address all of the questions the SM leaves unanswered and which can explain the values of the various input parameters (*e.g.*, fermion masses and mixing angles). Although there are many suggestions in the literature, no one truly knows the form this new physics might take or how it may first manifest itself. Instead of the direct production of new particles, physics beyond the SM may first appear as deviations in observables away from SM expectations, such as in the rates for rare processes or in precision electroweak tests. Another possibility is that deviations of order unity may be observed in cross sections once sufficiently high energy scales are probed. This kind of new physics can generally be parameterized via a finite set of non-renormalizable contact interactions, an approach which has been quite popular in the literature[2] for many years.

In this paper we will explore the capability of both the Tevatron and LHC, as well as possible future $\sqrt{s}$=60 and 200 TeV hadron colliders, to probe for the existence of flavor-independent(apart from electric charge), $q\bar{q}\gamma\gamma$ contact interactions of dimension-8. This is the lowest dimension gauge invariant operator involving two fermions as well as two photons. The observation of the signatures associated with the existence of this operator, which are discussed below, would be a clear signal of compositeness. Searches for such operators, with the quarks replaced by electrons, *i.e.*, $e^+e^-\gamma\gamma$ contact interactions, have already been performed at LEP1.5 [3] and have resulted in a lower bound of approximately 170 GeV on the associated mass scale. This constraint is not far above LEP's center of mass energy. Since this possibility has been explored for the Tevatron and LHC previously[4], we refer the reader to earlier work for details in these two cases. As we will see below, the Tevatron(LHC) with an integrated luminosity of 2(100) fb^{-1} will easily be able to push the scale in the corresponding $q\bar{q}\gamma\gamma$ situation above to $\simeq 0.7(2.8)$ TeV with even larger scales accessible at the higher energy hadron machines or with increased luminosity.

To be definitive, we will follow the notation employed by [5] as well as by the LEP collaborations and assume that these new interactions are parity and CP conserving. In this case we can parameterize the lowest dimensional $q\bar{q}\gamma\gamma$ contact interaction as

$$\mathcal{L} = \frac{2ie^2}{\Lambda^4}Q_q^2 F^{\mu\sigma}F_\sigma^\nu \bar{q}\gamma_\mu \partial_\nu q \,, \tag{1}$$

where e is the usual electromagnetic coupling, Q_q is the quark charge, and Λ is the associated mass scale. Note that we have pulled out an overall factor of e^2 as this represents the strength of the new interaction associated with the couplings of two photons to a pair of fermions, however one is not forced to follow this convention. We have chosen this particular form of the interaction as to be able to directly compare with the limits obtained at e^+e^- colliders. The most obvious manifestation of this new operator is to modify the conventional Born-level partonic $q\bar{q} \to \gamma\gamma$ differential cross section so that it now takes the form

$$\frac{d\hat{\sigma}}{dz} = Q_q^4 \frac{2\pi\alpha^2}{3\hat{s}} \left[\frac{1+z^2}{1-z^2} \pm 2\frac{\hat{s}^2}{4\Lambda_\pm^4}(1+z^2) \right.$$

2

$$+ \left(\frac{\hat{s}^2}{4\Lambda_\pm^4} \right)^2 (1 - z^4) \Bigg] \, , \tag{2}$$

where $\hat{s}$, z are the partonic center of mass energy and the cosine of center of mass scattering angle, θ^*, respectively. Note that we have written $\Lambda_\pm$ in place of Λ in the equation above to indicate that the limits we obtain below will depend upon whether the new operator constructively or destructively interferes with the SM contribution. This is also reflected by the choice of sign in the cross term in the above expression for the parton-level cross section.
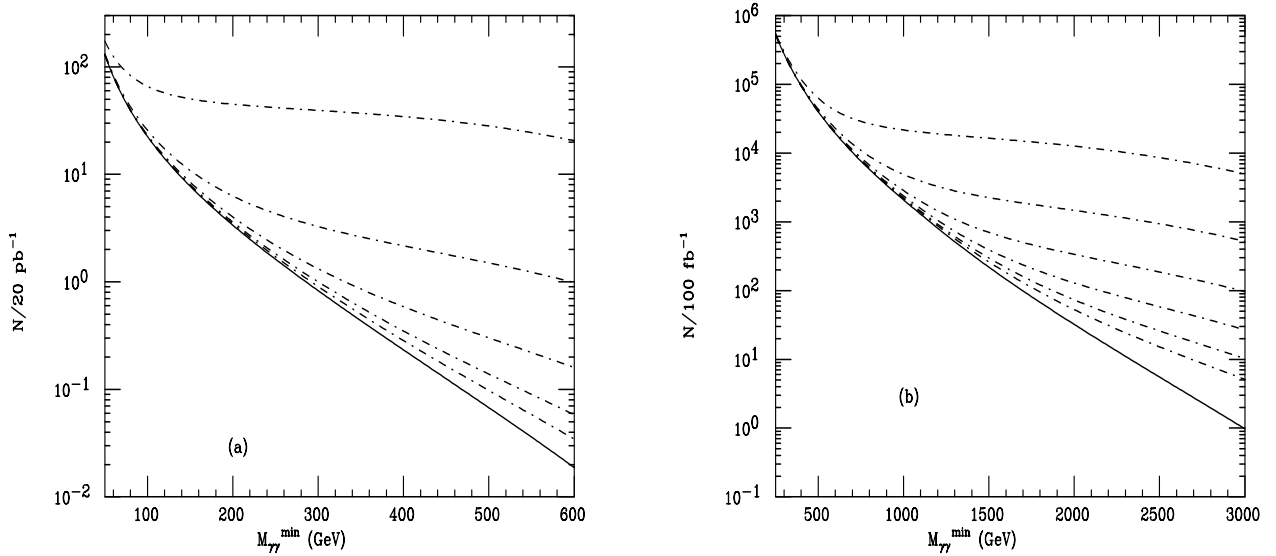

Figure 1: (a)Diphoton pair event rate, scaled to an integrated luminosity of $20pb^{-1}$, as a function of $M_{\gamma\gamma}^{min}$ at the 1.8 TeV Tevatron subject to the cuts $p_t^\gamma > 15$ GeV and $|\eta_\gamma| < 1$. The solid curve is the QCD prediction, while from top to bottom the dash dotted curves correspond to constructive interference with the SM and a compositeness scale associated with the $q\bar{q}\gamma\gamma$ operator of $\Lambda_+ = 0.2$, 0.3, 0.4, 0.5, and 0.6 TeV respectively. (b) Same as (a), but for the LHC scaling to an integrated lumonosity of $100fb^{-1}$. From top to bottom the dash dotted curves now correspond to $\Lambda_+ = 0.75$, 1.0, 1.25, 1.5, 1.75 and 2.0 TeV respectively. Here we require instead $p_t^\gamma > 200$ GeV and $|\eta_\gamma| < 1$.

2 Contact Interaction Effects

There are two major effects due to finite Λ: (i) Clearly, once $\hat{s}$ becomes even remotely comparable to Λ^2, the parton-level diphoton differential cross section becomes less peaked in the forward and backward directions implying that the photon pair will generally be more

central and will occur with higher average values of p_t. (*ii*) When integrated over parton distributions the resulting cross section will lead to an increased rate for photon pairs with large $\gamma\gamma$ invariant masses. From these two observations we see that the best hope for isolating finite Λ contributions is to look for excess diphotons with high, balanced p_t's in the central detector region with large pair masses. To take advantage of the fact that the sensitivity to the new contact interaction is greatest in the cental region we will demand both photons satisfy $|\eta_\gamma| \leq 1$ and apply increasingly strong p_t cuts on both photons as the collider center of mass energy increases. We will then examine the sensitivity to finite $\Lambda_\pm$ as a function of a lower cut placed on the $\gamma\gamma$ invariant mass, $M_{\gamma\gamma}^{min}$. This follows the basic procedure in our earlier analysis in Ref.[4].
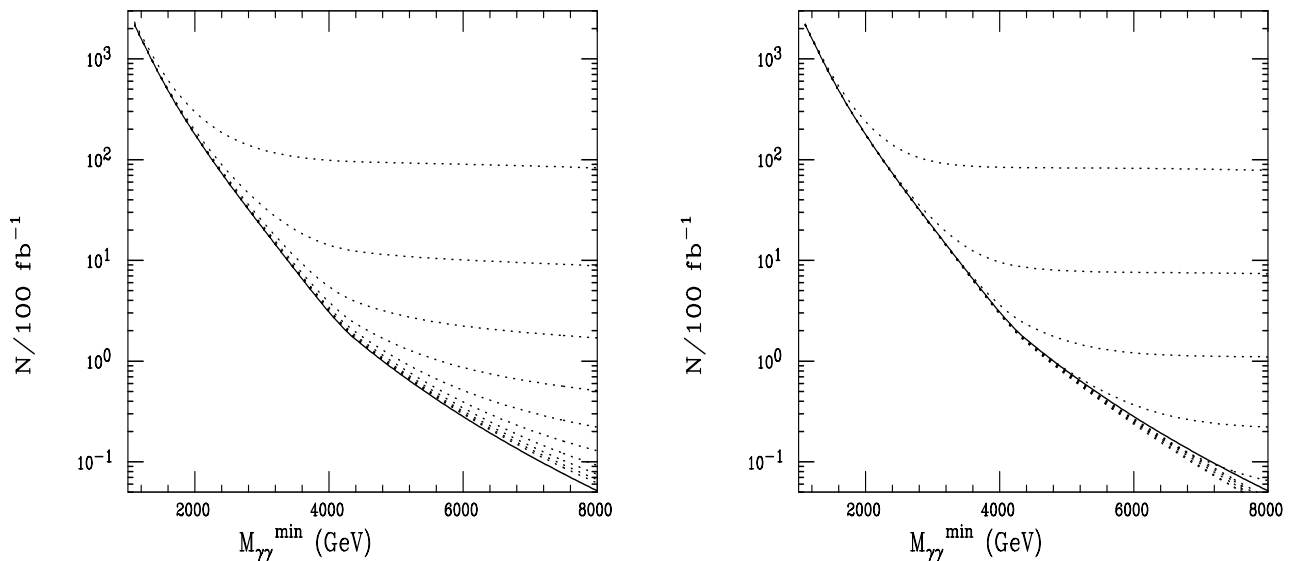

Figure 2: Event rate for isolated $\gamma\gamma$ events with invariant masses larger than $M_{\gamma\gamma}^{min}$ at a 60 TeV pp collider scaled to a luminosity of 100 fb^{-1}. The solid curve is the SM case while the top dotted curve corresponds to $\Lambda_+(\Lambda_-) = 3$ TeV in the left(right) figure. Each subsequent dotted curve corresponds to an increase in $\Lambda_\pm$ by 1 TeV. In either case we have applied the cuts $p_t^\gamma \geq 500$ GeV and $|\eta_\gamma| \leq 1$.

Unfortunately, the $q\bar{q} \rightarrow \gamma\gamma$ tree-level process is not the only one which produces diphotons that can satisfy the above criteria. The authors of Ref.[6] have provided an excellent summary of the various sources which lead to diphoton pairs and we will generally follow their discussion. The most obvious additional source of diphotons arises from the process $gg \rightarrow \gamma\gamma$ which is induced by box diagrams. Although relatively small in rate at the Tevatron, the increased gg luminosity as one goes to LHC (or higher) energies, combined with the fact that $q\bar{q}$ annihilation is now a 'sea-times-valence' process at pp colliders, implies that the subprocess $gg \rightarrow \gamma\gamma$ will be extremely important there.

4

We include the $gg-$induced diphotons in our calculations by employing 5 active quark flavors in the gg-induced box diagram for partonic center of mass energies, $\hat{s}$, below $4m_t^2$, 6 active flavors for $\hat{s} >> 4m_t^2$, and smoothly interpolate between these two cases. In order to include the potential effects of loop corrections to the rate for $gg \to \gamma\gamma$, we have scaled the results obtained by this procedure by an approximate 'K-factor' of 1.3(1.5) at the Tevatron(LHC and higher energy colliders). A similar 'K-factor' is also employed in the $q\bar{q} \to \gamma\gamma$ calculation; we use the results of Barger, Lopez and Putikka in Ref.[7]. While this procedure gives only an approximate result in comparison to the full NLO calculation, it is sufficient for our purposes since the effects of the new contact interaction are quite large as they directly modify the tree level cross section.
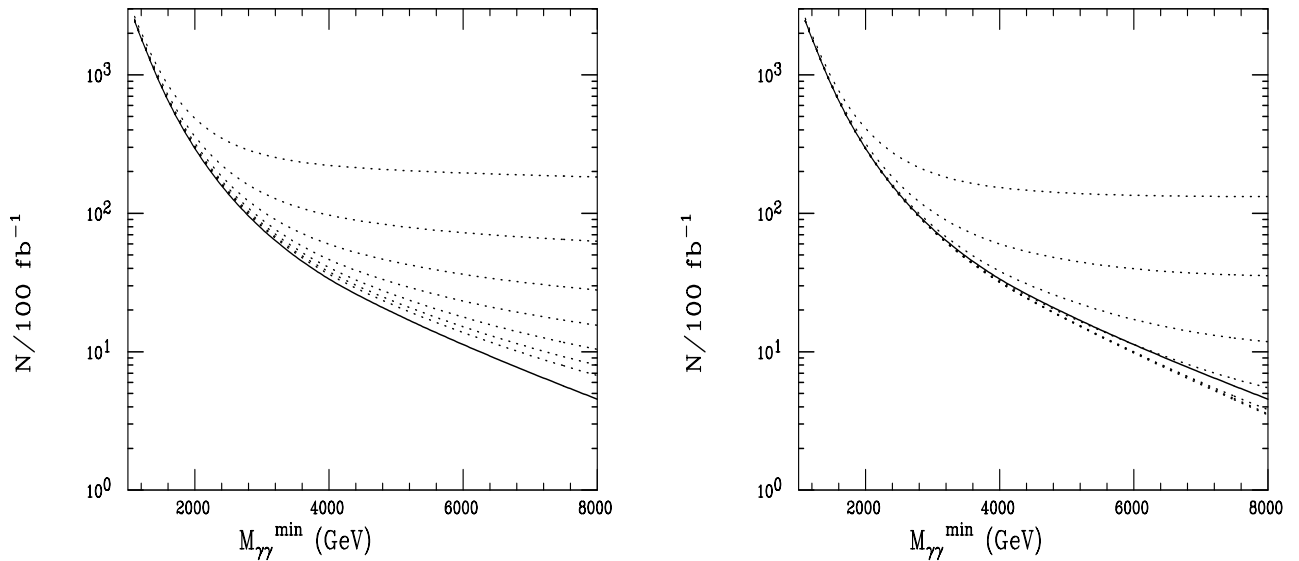

Figure 3: Same as the previous figure but now for the $p\bar{p}$ collision mode. The solid curve is the SM case while the top dotted curve corresponds to $\Lambda_+(\Lambda_-) = 8$ TeV in the left(right) figure. Each subsequent dotted curve corresponds to an increase in $\Lambda_\pm$ by 1 TeV.

Additional 'background' diphotons arise from three other sources. For $2 \to 2$ processes, one can have either (i) single photon production through $gq \to \gamma q$ and/or $q\bar{q} \to g\gamma$ followed by the fragmentation $g, q \to \gamma$, or (ii) a conventional $2 \to 2$ process with *both* final state q, g partons fragmenting to photons. Although these processes appear to be suppressed by powers of α_s, these are off-set by large logs. For $2 \to 3$ processes, (iii) double bremsstrahlung production of diphotons is possible, *e.g.*, $gq \to q\gamma\gamma$ or $q\bar{q} \to g\gamma\gamma$. All of these 'backgrounds' are relatively easy to drastically reduce or completely eliminate by a series of isolation cuts and by demanding p_t balancing between the two photons, which we require to be back to back in their center of mass frame.
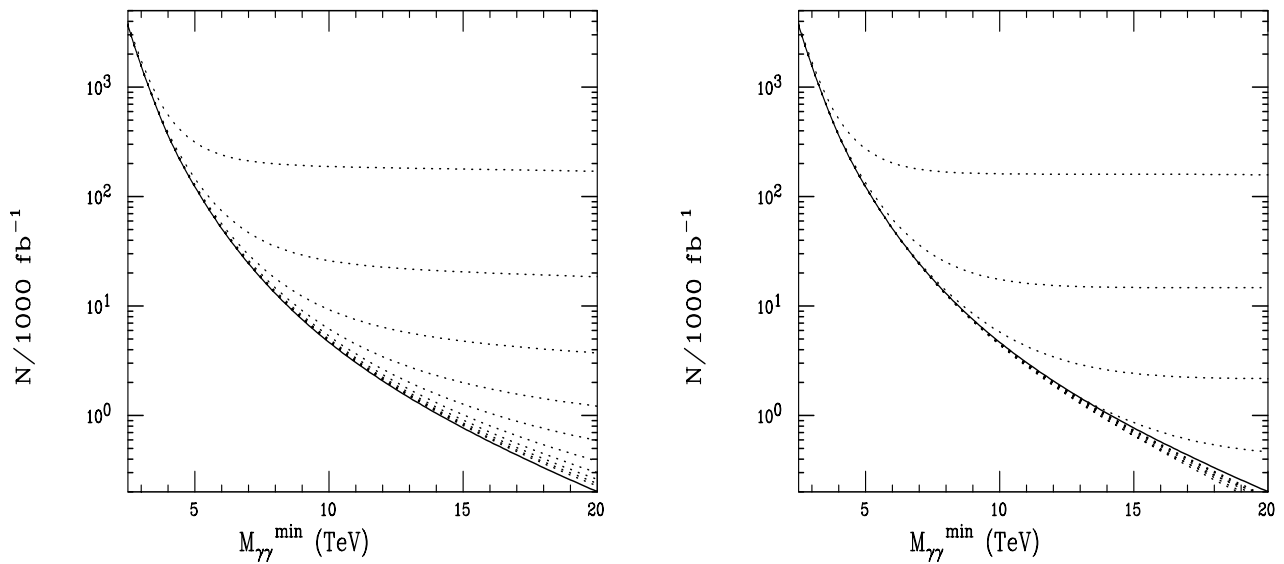
5

Figure 4: Event rate for isolated $\gamma\gamma$ events with invariant masses larger than $M_{\gamma\gamma}^{min}$ at a 200 TeV pp collider scaled to a luminosity of 1000 fb^{-1}. The solid curve is the SM case while the top dotted curve corresponds to $\Lambda_+(\Lambda_-) = 6$ TeV in the left(right) figure. Each subsequent dotted curve corresponds to an increase in $\Lambda_\pm$ by 3 TeV. In either case we have applied the cuts $p_t^\gamma \geq 1$ TeV and $|\eta_\gamma| \leq 1$.

3 Results

To obtain our results we fold the two parton-level subprocess cross sections with their associated parton densities, scale by appropriate K-factors and machine luminosities and then integrate over the relevant kinematic domain, subject to the appropriate cuts on both p_t and η_γ. We then obtain the number of events with the diphoton pair invariant mass larger than $M_{\gamma\gamma}^{min}$, which we display for different values of $\Lambda_\pm$ appropriate to the collider's center of mass energy. The results for the Tevatron and LHC can be seen in Fig. 1. Fig. 1a compares the SM diphoton cross section as a function of $M_{\gamma\gamma}^{min}$ with the constructive interference scenario for various values of Λ. It is clear that present data from the Tevatron is already probing values of Λ of order 400-500 GeV.
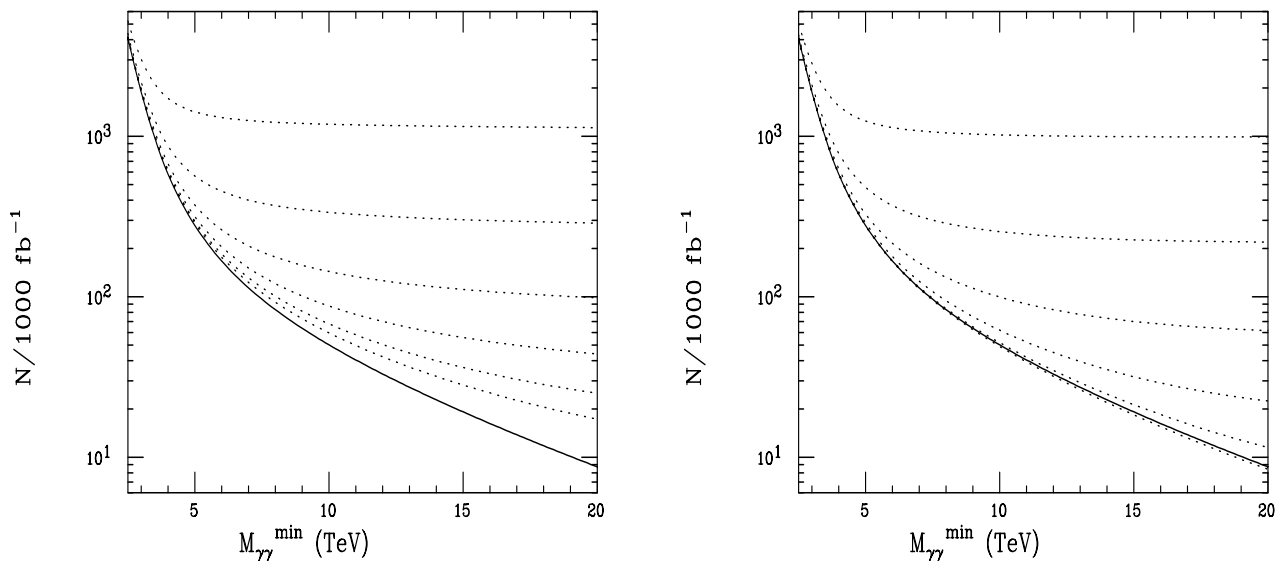

Figure 5: Same as the previous figure but now for the $p\bar{p}$ collision mode. The solid curve is the SM case while the top dotted curve corresponds to $\Lambda_+(\Lambda_-) = 15$ TeV in the left(right) figure. Each subsequent dotted curve corresponds to an increase in $\Lambda_\pm$ by 3 TeV.

Assuming that no event excesses are observed, one can ask, *e.g.*, for the limits that can be placed on $\Lambda_\pm$ as the Tevatron integrated luminosity is increased. This was done in our earlier analysis[4] by performing a Monte Carlo study. First the $M_{\gamma\gamma}^{min}$ range above 100 GeV was divided into nine bins of 50 GeV. Almost all of the sensitivity to finite Λ lies in this range since for smaller values of $M_{\gamma\gamma}^{min}$ the cross section looks very similar to the SM, while for larger values of $M_{\gamma\gamma}^{min}$ the event rate is too small to be useful even for integrated luminosities well in excess of a few fb^{-1}. Events were generated using the SM as input and the resulting $M_{\gamma\gamma}^{min}$ distribution was fit to a $\Lambda_\pm$-dependent fitting function. From this, bounds on Λ are directly obtainable via a χ^2 analysis. In this approach, it was assumed that the normalization

of the cross section for small values of $M_{\gamma\gamma}^{min}$ using experimental data will remove essentially all of the systematic errors associated with the cross section normalization. Hence, only statistical errors are used into the fitting procedure. Extending this approach to the case of $\sqrt{s}$=2 TeV Tevatron we obtains bounds on $\Lambda_\pm$ in excess of 0.7 TeV as shown in Table I. Note that the constraints we obtain on Λ_- will generally be weaker than those for Λ_+. Increasing the integrated luminosity at the Tevatron by another factor of ten as is proposed in the TeV33 study, will most likely push these constraints upwards by approximately 200 GeV.

At the LHC, we find the results presented in Fig. 1b which clearly shows that values of Λ greater than 2 TeV will be easily probed. If one follows the same Monte Carlo approach as above, one obtains very strong limits on $\Lambda_\pm$. Here the $M_{\gamma\gamma}^{min}$ range above 250 GeV is divided into ten bins and data is generated as above and subsequently fitted to a $\Lambda_\pm$-dependent distribution. From this analysis we obtain the 95% CL bounds of $\Lambda_+ > 2.83$ TeV and $\Lambda_- > 2.88$ TeV as displayed in Table I. If we increase the integrated luminosity to $200 fb^{-1}$, these limits are found to increase to $\Lambda_+ > 3.09$ TeV and $\Lambda_- > 3.14$ TeV. It is interesting to note that if we relax the η^γ cuts at the LHC (from 1 to 2.5) we get an increase in statistics but a loss of sensitivity. These two effects essentially cancel in this case yielding essentially the same bounds as shown in the Table. Note that in the case of the LHC we obtain comparable sensitivities to both Λ_+ and Λ_-.

Machine	p_t^{min}(GeV)	$|\eta_{\gamma,max}|$	$\mathcal{L}$	Λ_+	Λ_-
TeV	15	1	2	0.75	0.71
LHC	200	1,2.5	100	2.8	2.9
60 TeV (pp)	500	1	100	$\simeq 9.5$	$\simeq 6.5$
60 TeV ($p\bar{p}$)	500	1	100	$\simeq 13.5$	$\simeq 10.5$
200 TeV (pp)	1000	1	1000	$\simeq 23$	$\simeq 16$
200 TeV ($p\bar{p}$)	1000	1	1000	$\simeq 33$	$\simeq 26$

Table 1: 95% CL bounds on the scale of the $q\bar{q}\gamma\gamma$ contact interaction at future hadron colliders. Note the greater sensitivity at $p\bar{p}$ in comparison to pp colliders of the same center of mass energy. Here, $\mathcal{L}$ is the machine integrated luminosity in fb^{-1} and $\Lambda_\pm$ are in units of TeV.

Turning our attention to the higher energy $\sqrt{s}$=60 and 200 TeV machines, we can now explore the differences in sensitivity to pp versus $p\bar{p}$ initial states. Clearly we anticipate larger sensitivities in the $p\bar{p}$ case since the $q\bar{q}$ process is now proportional to valence times valence distributions instead of valence times sea. For the 60 TeV collider our results are shown in Figures 2 and 3 assuming an integrated luminosity of 100 fb^{-1}. As in the Tevatron case we see that there is somewhat greater sensitivity in the case of constructive interference(Λ_+) than in the case of destructive interference(Λ_-). Also, as anticipated, the larger $q\bar{q}$ cross section at the $p\bar{p}$ collider results in substantially enhanced sensitivity with an approximate

40% increase in reach for Λ_+ and an approximate 60% increase in reach for Λ_-. Table I summarizes these approximate results; full Monte Carlo studies along the lines discussed above for the Tevatron and LHC have not yet been completed.

At $\sqrt{s}$=200 TeV this pattern is essentially repeated as can be seen from Figures 4 and 5 as well as Table I where an integrated luminosity of 1000 fb^{-1} has now been assumed. Note that the 'reach' in Λ sensitivity does not scale linearly with the collider energy.

Excess diphoton events should be searched for, not only as narrow peaks in $M_{\gamma\gamma}$ signalling the existence of Higgs-like objects, but also in the broad contributions to the tails of distributions. Such searches may yield valuable information on the existence of new physics.

4   Acknowledgements

References

[1] A. Blondel, plenary talk given at the *28th International Conference on High Energy Physics*, Warsaw, Poland, 25-31 July 1996.

[2] See, for example, E. Eichten, K. Lane and M. Peskin, Phys. Rev. Lett. **50**, 811 (1983); B. Schrempp, F. Schrempp, N. Wermes and D. Zeppenfeld, Nucl. Phys. **B296**, 1 (1988).

[3] D. Buskulic *et al.*, ALEPH Collaboration, CERN report CERN-PPE/96-53, 1996; F. Barao *et al.*, DELPHI Collaboration, DELPHI report DELPHI 96-125, 1996; M. Acciarri *et al.*, L3 Collaboration, CERN report CERN-PPE/96-48, 1996; G. Alexander *et al.*, OPAL Collaboration, CERN report CERN-PPE/96-39, 1996.

[4] T.G Rizzo, Phys. Rev. **D51**, 1064 (1994).

[5] See, for example, P. Méry, M. Perrottet and F.M. Renard, Z. Phys. **C38**, 579 (1988).

[6] B. Bailey, J.F. Owens, and J. Ohnemus, Phys. Rev. **D46**, 2018 (1992); J. Ohnemus and J.F. Owens, Phys. Rev. **D43**, 3626 (1991); see also, P. Aurenche *et al.*, Nucl. Phys. **B286**, 553 (1987).

[7] V. Barger, J.L. Lopez and W. Putikka, Int. J. Mod. Phys. **A3**, 2181 (1988); A.P. Contogouris, S. Papadopoulos and J.P. Ralston, Phys. Rev. **D25**, 1280 (1982); A.P. Contogouris and H. Tanaka, Phys. Rev. **D33**, 1265 (1986); N. Mebarki and H. Tanaka, Mod. Phys. Lett. **A2**, 735 (1987); C.J. Gilmour, Cambridge University report DAMTP 84/19.